

Nanosecond Redox Equilibrium Method for Determining Oxidation Potentials in Organic Media

Gonzalo Guirado, Cavan N. Fleming, Thor G. Lingenfelter, Michelle L. Williams, Han Zuilhof,[†] and Joseph P. Dinnocenzo*

Contribution from the Department of Chemistry and the Center for Photoinduced Charge Transfer, University of Rochester, Rochester, New York 14627-0216

Received May 24, 2004; E-mail: jpd@chem.rochester.edu

Abstract: A general, nanosecond equilibrium method is described for determining thermodynamically meaningful oxidation potentials in organic media for compounds that form highly reactive cation radicals upon one-electron oxidation. The method provides oxidation potentials with unusually high precision and accuracy. Redox ladders have been constructed of appropriate reference compounds in dichloromethane and in acetonitrile that can be used to set up electron-transfer equilibria with compounds with unknown oxidation potentials. The method has been successfully applied to determining equilibrium oxidation potentials for a series of aryl-alkylcyclopropanes, whose oxidation potentials were imprecisely known previously. Structure-property trends for oxidation potentials of the cyclopropanes are discussed.

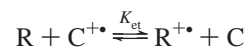
Introduction

Accurate oxidation potentials provide important data for evaluating a variety of thermodynamic properties of organic cation radicals (e.g., bond dissociation energies and pK_a 's).¹ Unfortunately, for compounds that form reactive cation radicals upon one-electron oxidation, the most common method of obtaining oxidation potentials—cyclic voltammetry with millimetric electrodes—often fails to provide reversible voltammetric data. One solution to this problem has been provided by the introduction of ultramicroelectrodes, which decrease the electrochemical cell response time and ohmic (iR) drop, thereby permitting significantly higher scan rates to be used.² Potentiostats that operate in the megavolt per second range have recently been demonstrated which, in principle, allow oxidation potentials to be measured for compounds whose corresponding ion radicals have lifetimes in the nanosecond regime.³ Despite these impressive advances in ultrafast cyclic voltammetry instrumentation, full advantage of the technique can be realized only for substrates that have extremely high heterogeneous rates for electron transfer at the electrode. Unfortunately, this criterion is not met by many substrates.

Redox catalysis provides an alternative and powerful, indirect electrochemical technique for estimating redox potentials of

compounds that form highly reactive ion radicals.^{2b,4} The method utilizes an electron-transfer mediator that undergoes rapid and reversible electron transfer at an electrode. The reduced (or oxidized) mediator then undergoes electron transfer with the substrate of interest. In turn, the substrate ion radical undergoes follow-up reaction(s) in competition with return electron transfer to the mediator. Experimentally, the standard potential for reduction (oxidation) of the substrate is obtained from an extrapolated plot of the homogeneous rate constants for reduction (oxidation) of a range of mediators vs the standard potentials of the mediators. Although this method can, in principle, be applied to both reductive and oxidative chemistry, it has rarely been used to determine standard oxidation potentials,⁵ presumably due to the lack of suitable mediators that are rapidly and reversibly oxidized under standard electrochemical conditions, especially at relatively high potentials.

Herein we describe a complementary approach to modern electrochemical methods for determining accurate oxidation potentials of compounds that form reactive cation radicals. The technique utilizes nanosecond transient absorption spectroscopy to monitor the electron-transfer equilibrium established between a reference compound (R) of known oxidation potential and a compound of unknown oxidation potential (C), i.e.,



Historically, Patel and Wilson first used the equilibrium electron-transfer method in a transient experiment to measure the equilibrium constant for electron exchange between super-

[†] Current address: Department of Organic Chemistry, Wageningen University, Dreijenplein 8, 6703 HB Wageningen, The Netherlands.

- (1) See, for example: (a) Okamoto, A.; Snow, M. S.; Arnold, D. R. *Tetrahedron* **1986**, *42*, 6175. (b) Popielarz, R.; Arnold, D. R. *J. Am. Chem. Soc.* **1990**, *112*, 3068. (c) Wayner, D. D. M.; Parker, V. D. *Acc. Chem. Res.* **1993**, *26*, 287. (d) Maslak, P.; Vallombroso, T. M.; Chapman, W. H., Jr.; Narvaez, J. N. *Angew. Chem., Int. Ed. Engl.* **1994**, *33*, 73.
- (2) (a) Wightman, R. M.; Wipf, D. O. *Electroanal. Chem.* **1989**, *15*, 267. (b) Andrieux, C. P.; Hapiot, P.; Savéant, J.-M. *Chem. Rev.* **1990**, *90*, 723. (c) Heinze, J. *Angew. Chem., Int. Ed. Engl.* **1993**, *32*, 1268. (d) Amatore, C.; Bourret, Y.; Maisonhaute, E.; Abruna, H. D.; Goldsmith, J. I. C. R. *Chim.* **2003**, *6*, 99.
- (3) (a) Amatore, C.; Maisonhaute, E.; Simmoneau, G. *Electrochem. Commun.* **2000**, *2*, 81. (b) Amatore, C.; Maisonhaute, E.; Simmoneau, G. *J. Electroanal. Chem.* **2000**, *486*, 141.

(4) Andrieux, C. P.; Savéant, J.-M. *Electrochemical Reactions*. In *Investigation of Rates and Mechanisms of Reactions*; Bernasconi, C. P., Ed.; Techniques of Chemistry 6; Wiley-Interscience: New York, 1986; Part 2, p 305.

(5) (a) Anne, A.; Mioroux, J.; Savéant, J.-M. *J. Am. Chem. Soc.* **1993**, *115*, 10224. (b) Keita, B.; Essaadi, K.; Nadjo, L.; Contant, R.; Justum, Y. *J. Electroanal. Chem.* **1996**, *404*, 271.

oxide anion radical and duroquinone.⁶ The method has been used in subsequent pulse radiolysis studies to estimate reduction potentials for a variety of inorganic and organic compounds.⁷ Prior investigations have largely been restricted to work in protic media due to the ease of generating solvated electrons in these solvents.⁸ Many cation radicals are unstable in these media, however, due to proton transfer to and/or nucleophilic attack by the solvents. A general method for measuring oxidation potentials in nonbasic and nonnucleophilic organic solvents by using the electron-transfer equilibrium method is currently lacking and would clearly be desirable.

In connection with recent work in our laboratory on the chemistry of arylcyclopropane cation radicals,⁹ we required the oxidation potentials of the corresponding neutral cyclopropanes to estimate bond dissociation energies and to construct linear free energy relationships. Electrochemical oxidations of the cyclopropanes were irreversible due to rapid follow-up reactions of their cation radicals, including nucleophilic attack by the solvent (CH₃CN). The irreversible nature of the electrochemical oxidations led to unacceptably large uncertainties in the derived potentials. For example, literature oxidation potentials for phenylcyclopropane vary from 1.72 to 2.34 V vs SCE (vide infra)—a range of >14 kcal/mol! Obviously, this large uncertainty compromises the use of electrochemically derived oxidation potentials for estimating thermodynamic properties. We therefore sought to develop a reliable method for determining the oxidation potentials of arylcyclopropanes by equilibrium electron transfer with suitable reference compounds in non-nucleophilic organic solvents. As will become clear, the method has broad utility for the determination of oxidation potentials of compounds that lead to reactive cation radicals.

Results and Discussion

To set up the electron-transfer equilibrium, photoinduced electron transfer was selected as the method of choice for cation radical generation since it provides flexibility with respect to the reaction medium.

A. Photooxidation System. Four primary criteria were identified for the photooxidation system:

(i) The photosensitizer must absorb at sufficiently long wavelength such that competitive absorption does not occur by the arylcyclopropanes or the reference compounds.

(ii) Each laser pulse that excites the photosensitizer should generate the same total concentration of cation radicals, in high quantum yield, regardless of the oxidation potentials of the arylcyclopropanes and the reference compounds. This criterion ensures that spectra of the pure arylcyclopropane and reference cation radicals properly reflect their relative extinction coef-

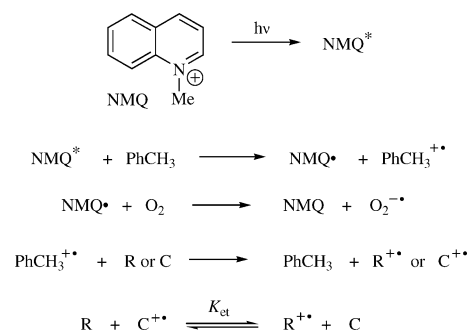
ficients, which is essential for accurate fitting of the electron-transfer equilibrium spectra.

(iii) It should be possible to generate the cation radicals in relatively nonnucleophilic solvents (e.g., CH₂Cl₂), since many arylcyclopropanes rapidly react with polar nucleophilic solvents like acetonitrile.⁹

(iv) The absorption spectrum of the one-electron-reduced photosensitizer should not interfere with the cation radical absorptions of the arylcyclopropanes or the reference compounds.¹⁰

All of these criteria were met by a photooxidant system consisting of *N*-methylquinolinium hexafluorophosphate (NMQ) as photosensitizer, toluene (1 M) as codonor, and CH₂Cl₂ as solvent.^{9f,11} This system has a number of advantages. NMQ can be conveniently excited at sufficiently long wavelength (343 nm) so that there is no competitive absorption by the arylcyclopropanes or the reference compounds. In addition, the singlet excited state of NMQ is a powerful one-electron oxidant ($E_{\text{red}} = 2.7$ V vs SCE). Using toluene in high concentration as a codonor leads to initial formation of the NMQ^{*}/PhCH₃⁺⁺ geminate radical/cation-radical pair, which undergoes efficient separation even in moderate polarity solvents like dichloromethane.¹² The “free” toluene cation radical is a powerful one-electron oxidant ($E_{\text{red}} = 2.35$ V vs SCE)¹³ that can then be used to effectively, irreversibly oxidize the arylcyclopropanes (C) and reference (R) compounds that are present at relatively low concentration (e.g., 1–50 mM) in solution. Thus, in a pulsed laser experiment, each laser pulse produces the same concentration of PhCH₃⁺⁺ and, consequently, the same total concentration of arylcyclopropanes and reference cation radicals. Importantly, the reduced form of the photooxidant, NMQ^{*}, can be rapidly scavenged with dioxygen, leading to O₂^{•-}, which does not have interfering absorptions in the UV–vis region where many organic cation radicals strongly absorb. Working under dioxygen-saturated conditions does not interfere with the observation of organic cation radicals since most of them do not react rapidly with dioxygen.¹⁴ The primary processes of the overall photooxidant scheme are illustrated in Scheme 1.

Scheme 1

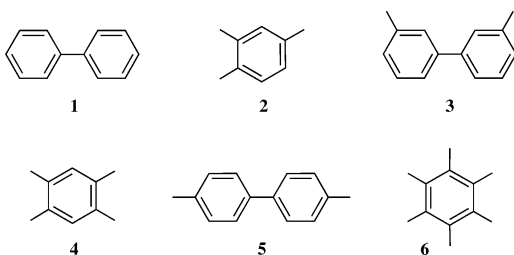


B. Selection of Reference Compounds. On the basis of cyclic voltammetry experiments, the oxidation potentials of the

- (6) Patel, K. B.; Wilson, R. L. *J. Chem. Soc., Faraday Trans. 1* **1973**, 69, 814.
 (7) For reviews, see: (a) Wardman, P. *J. Phys. Chem. Ref. Data* **1989**, 18, 1637. (b) Stanbury, D. M. In *General Aspects of the Chemistry of Radicals*; Alfassi, Z. B., Ed.; Wiley: New York, 1999, Chapter 11.
 (8) For rare exceptions, see: (a) Gould, I. R.; Ege, D.; Moser, J. F.; Farid, S. *J. Am. Chem. Soc.* **1990**, 112, 4290. (b) Simpson, T. R. Ph.D. Dissertation, University of Rochester, Rochester, NY, 1994.
 (9) (a) Dinnocenzo, J. P.; Conlon, D. A. *J. Am. Chem. Soc.* **1988**, 110, 2324. (b) Dinnocenzo, J. P.; Todd, W. P.; Simpson, T. R.; Gould, I. R. *J. Am. Chem. Soc.* **1990**, 112, 2462. (c) Dinnocenzo, J. P.; Lieberman, D. R.; Simpson, T. R. *J. Am. Chem. Soc.* **1993**, 115, 366. (d) Dinnocenzo, J. P.; Conlon, D. A. *Tetrahedron Lett.* **1995**, 36, 7415. (e) Karki, S. B.; Dinnocenzo, J. P.; Farid, S.; Goodman, J. L.; Gould, I. R.; Zona, T. A. *J. Am. Chem. Soc.* **1997**, 119, 431. (f) Dinnocenzo, J. P.; Simpson, T. R.; Zuilhof, H.; Todd, W. P.; Heinrich, T. *J. Am. Chem. Soc.*, **1997**, 119, 987. (g) Dinnocenzo, J. P.; Zuilhof, H.; Lieberman, D. R.; Simpson, T. R.; McKechney, M. W. *J. Am. Chem. Soc.* **1997**, 119, 994.

- (10) This requirement is necessary only if one intends to record clean cation radical spectra of both species involved in the electron-transfer equilibrium.
 (11) Dockery, K. P.; Dinnocenzo, J. P.; Farid, S.; Goodman, J. L.; Gould, I. R.; Todd, W. P. *J. Am. Chem. Soc.* **1997**, 119, 1877.
 (12) Todd, W. P.; Dinnocenzo, J. P.; Farid, S.; Goodman, J. L.; Gould, I. R. *J. Am. Chem. Soc.* **1991**, 113, 3601.
 (13) Schlesener, C. J.; Amatore, C.; Kochi, J. K. *J. Phys. Chem.* **1986**, 90, 3747.
 (14) It is not essential to remove NMQ^{*} to perform equilibrium measurements. It is does, however, permit cation radical spectra to be measured without interference by absorptions due to NMQ^{*}.

arylcyclopropanes we intended to measure by the redox equilibrium method were estimated to be in the range of ~ 1.5 – 2.0 V vs SCE. Thus, it was immediately clear that no single reference compound could be used to measure all of the electron-transfer equilibrium constants with the arylcyclopropanes since, otherwise, extremely large concentration differences would be required to achieve comparable absorptions of both the reference and cyclopropane cation radicals. This, in turn, would increase the time necessary to achieve the redox equilibrium and result in diminution of the cation radical absorptions due to various decay pathways for the cation radicals (e.g., return electron-transfer processes or reaction with adventitious nucleophiles and/or electron donor impurities). Thus, a range of reference compounds whose oxidation potentials spanned this redox range were needed in order to construct a redox ladder. The choice of the reference compounds was dictated by several criteria. In addition to spanning the above redox range, the reference compounds should be readily available, they should form relatively stable cation radicals, and the cation radicals should exhibit reasonably strong absorptions in the visible region of the spectrum. It was also important that the cation radicals of adjacent pairs of reference compounds along the redox ladder absorb in different regions of the visible spectrum. Finally, the differences in the oxidation potentials of adjacent pairs of reference compounds needed to be reasonably small (≤ 0.1 V), for the reason cited above. Fortunately, we found that all of these criteria could be met with appropriate combinations of alkyl-substituted benzenes and biphenyls. The oxidation potentials of these compounds can be readily tuned over the potential range of interest by alkyl substitution and give rise to relatively stable cation radicals that conveniently absorb in different spectral regions (alkylbenzene cation radicals, 450–500 nm; biphenyl cation radicals, 670–700 nm). In practice, we used the six reference compounds shown below, which are arranged in order of decreasing oxidation potential.



Before measuring the absorption spectra for the cation radicals of the reference compounds, it was necessary to determine the lifetime of NMQ^{\bullet} in a dioxygen-saturated solution to ensure that the spectrum of NMQ^{\bullet} would not interfere with the cation radical spectra. First, a spectrum of NMQ^{\bullet} was generated by adding benzytrimethylsilane (0.05 M) to the above photooxidant system in an argon-saturated CH_2Cl_2 solution. Under these conditions, $\text{PhCH}_2\text{SiMe}_3$ has been shown to react with $\text{PhCH}_3^{+\bullet}$ to produce $\text{PhCH}_2\text{SiMe}_3^{+\bullet}$, which undergoes rapid fragmentation (< 50 ns) to form products that are optically transparent in the visible region of the spectrum.¹¹ The absorption spectrum recorded 50 ns after the laser pulse (Figure 1) shows a long-lived species with $\lambda_{\text{max}} \approx 540$ nm, in good agreement with the literature value for NMQ^{\bullet} .¹⁵ The lifetime of NMQ^{\bullet} in dioxygen-

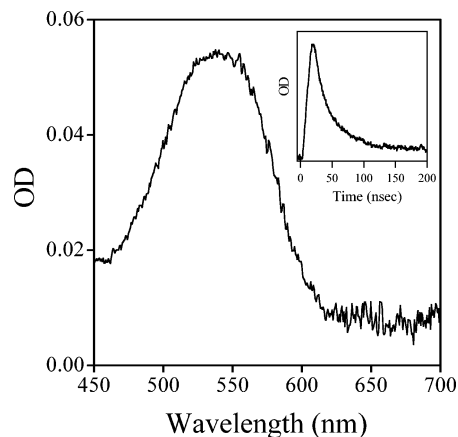


Figure 1. Transient spectrum of NMQ^{\bullet} recorded 100 ns after the laser pulse in argon-saturated CH_2Cl_2 . Inset shows transient kinetic trace in dioxygen-saturated solution monitoring at 540 nm.

saturated CH_2Cl_2 solution was next measured by transient kinetics. The inset of Figure 1 shows a transient kinetic trace monitoring at 540 nm, which shows that NMQ^{\bullet} reacts nearly completely with O_2 within ~ 100 ns. Similar results were obtained in CH_3CN .

Spectra for the cation radicals of **1**–**6** were generated using the NMQ/PhCH_3 photooxidant system for concentrations of the reference compounds ranging from 0.005 to 0.05 M. Over this concentration range, the growth of the cation radicals of the reference compounds was complete in ≤ 50 ns. Spectra were typically recorded at ≥ 100 ns, however, to allow for decay of NMQ^{\bullet} . The experimental spectra showed that the optical densities for each of the cation radical absorptions at their λ_{max} were invariant to the concentration of the neutral reference compound, except in the case of **6**. In this case, the absorbance at λ_{max} for $\mathbf{6}^{+\bullet}$ was ~ 1.2 times greater at 0.005 M than at 0.05 M, in both CH_2Cl_2 and CH_3CN . We attribute the lower absorbance of $\mathbf{6}^{+\bullet}$ at higher [6] to formation of a small amount of dimer cation radical, i.e., $\mathbf{6}_2^{+\bullet}$, which absorbs outside our spectral region.¹⁶ Therefore, in this case, the spectrum of $\mathbf{6}^{+\bullet}$ used for fitting equilibrium spectra was generated at < 0.005 M **6**, where the dimer cation radical contributes $< 2\%$. Fortunately, for all redox equilibria involving **6**, it was possible to work at [6] < 0.005 M, so intrusion by $\mathbf{6}_2^{+\bullet}$ was negligible in our equilibrium experiments.¹⁷ Direct evidence that $\mathbf{6}_2^{+\bullet}$ does not interfere with oxidation potential measurements was derived from electron-transfer equilibrium measurements with **5**, where the equilibrium-derived difference in oxidation potentials between **5** and **6** was found to be in excellent agreement with that determined electrochemically (vide infra).

The fact that optical densities of the reference cation generated by the NMQ/PhCH_3 photooxidant system were invariant with concentration of the neutral reference compounds (except, of course, for **6**) demonstrates that **1**–**6** are effectively, irreversibly oxidized by $\text{PhCH}_3^{+\bullet}$. This conclusion is consistent with reported oxidation potential data. For biphenyl (**1**), the reference compound of highest oxidation potential, the difference in oxidation potential between PhCH_3 and **1** is ~ 0.4 V (~ 9 kcal/mol).¹⁸ Thus,

(16) Badger, B.; Brocklehurst, B. *Trans. Faraday Soc.* **1969**, *65*, 2582.

(17) A 2% formation of a dimer cation radical would result in a 2% error in the determination of K_{et} , which corresponds to an error in ΔE_{ox} of ~ 0.0005 V.

(18) Based on the oxidation potentials of toluene and biphenyl in refs 13 and 8a, respectively.

(15) Cozzens, R. F.; Gover, T. A. *J. Phys. Chem.* **1970**, *74*, 3003.

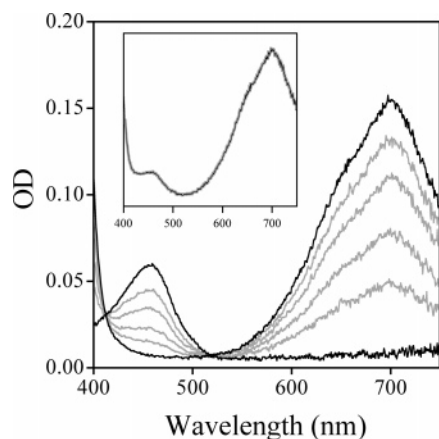
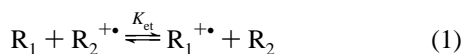


Figure 2. Spectra of durenene cation radical ($\lambda_{\text{max}} = 457$ nm), 3,3-dimethylbiphenyl cation radical ($\lambda_{\text{max}} = 700$ nm), and the corresponding equilibrium, electron-transfer spectra (gray lines) in CH_2Cl_2 . Inset shows one of the experimental spectra (gray line) and the best least-squares fit to it according to eq 2 (thin black line).

the equilibrium constant for electron transfer from **1** to $\text{PhCH}_3^{+\bullet}$ is $>10^6$ at 20 °C, the temperature of the equilibrium measurements. The electron-transfer equilibrium constants for the other reference compounds with $\text{PhCH}_3^{+\bullet}$ will, of course, be even greater.

Redox equilibrium spectra were recorded for pairs of the reference compounds at appropriate concentrations of the neutrals (typically between 1 and 50 mM) so that the spectra of both cation radicals could be detected.¹⁹ The approach to equilibrium was followed in each case by monitoring the absorptions of the cation radicals at their λ_{max} , and delay times sufficient to reach equilibrium were thereby chosen. The results for compounds **3** and **4**, which are typical, are shown in Figure 2. As can be seen, a clean isosbestic point is observed, as expected for the simple electron-transfer equilibrium in eq 1. The equilibrium constant was determined by least-squares fitting of the experimental spectra to eq 2,²⁰ where $A_{\text{m},i}$ is the absorbance of the equilibrium mixture at wavelength i , $A_{\text{R}_1,i}$ and $A_{\text{R}_2,i}$ are the absorbances of the cation radicals of reference compounds R_1 and R_2 at wavelength i , $[\text{R}_1]$ and $[\text{R}_2]$ are the concentrations of R_1 and R_2 , and K_{et} is the electron-transfer equilibrium constant. Typically, K_{et} was the only adjustable parameter in eq 2 that needed to be fit. From K_{et} , the difference in oxidation potential, $E_{\text{ox}}(\text{R}_1) - E_{\text{ox}}(\text{R}_2)$, was calculated from the Nernst equation (eq 3).



$$A_{\text{m},i} = A_{\text{R}_1,i} \left(\frac{K_{\text{et}}[\text{R}_1]}{[\text{R}_2] + K_{\text{et}}[\text{R}_1]} \right) + A_{\text{R}_2,i} \left(\frac{[\text{R}_2]}{[\text{R}_2] + K_{\text{et}}[\text{R}_1]} \right) \quad (2)$$

$$\Delta E_{\text{ox}} = E_{\text{ox}}(\text{R}_1) - E_{\text{ox}}(\text{R}_2) = -(RT/F) \ln K_{\text{et}} \quad (3)$$

When the difference in the oxidation potentials of the electron donors is large (~ 0.1 V), a relatively large concentration ratio of the neutrals is required to attain comparable absorbances for both cation radicals. In these cases, the concentrations of the high oxidation potential reference compound was kept <0.05

(19) In principle, K_{et} can be determined even if the absorption of only one of the cation radicals is detectable.

(20) Meisel, D.; Neta, P. *J. Am. Chem. Soc.* **1975**, *97*, 5198.

Table 1. Oxidation Potentials Differences for **1–6** Determined from Redox Equilibrium Experiments (ΔE_{ox}) at 20 °C, Oxidation Potentials for **1–6** ($E_{\text{ox}}^{\text{eq}}$) Based on ΔE_{ox} , and Electrochemically Determined Oxidation Potentials for **1–6** ($E_{\text{ox}}^{\text{el}}$) in CH_2Cl_2 and CH_3CN

compd	CH_2Cl_2		CH_3CN			
	ΔE_{ox}	($E_{\text{ox}}^{\text{eq}}$) ^a	($E_{\text{ox}}^{\text{el}}$) ^{a,b}	ΔE_{ox}		($E_{\text{ox}}^{\text{eq}}$) ^a
1		1.950(7)	1.96		1.953(6)	
2	0.025(1)	1.925(7)	1.92	0.048(3)	1.905(5)	
3	0.082(4)	1.843(6)	1.85	0.061(2)	1.844(4)	
4	0.071(2)	1.772(6)	1.78	0.091(1)	1.753(4)	1.75
5	0.108(3)	1.664(5)	1.66	0.083(3)	1.670(2)	
6	0.074(5)	1.590 ^d	1.59	0.090(2)	1.580 ^d	1.58

^a Oxidation potentials in V vs SCE; standard deviation in the last significant digit in parentheses. ^b Reference 8a. ^c Reference 22. ^d Value based on literature electrochemical data.

M, since otherwise it competitively intercepts NMQ^* , which lowers the overall quantum for cation radical formation and thus the total cation radical concentration. Consequently, a relatively low concentration of the low oxidation potential reference compound had to be used, which, in turn, resulted in longer delay times to reach equilibrium. As the delay time after the laser pulse was lengthened, the equilibration time sometimes became competitive with decay of the cation radical absorbances from return electron transfer, which leads to a lower total cation radical concentration at equilibrium. This process was easily detected experimentally and could be conveniently accounted for during fitting process by multiplying the right-hand side of eq 2 by a scaling factor during the fitting process, which introduced a second adjustable parameter. Since absorption spectra were typically recorded at >500 wavelengths, even when a scaling factor is introduced the number of observations used for fitting greatly exceeds the number of fitted parameters.

Equation 2 makes the conventional assumption that concentrations can be used in place of activity coefficients. Thus, the ΔE_{ox} values derived from the redox equilibrium experiments are strictly differences in formal potentials rather than standard potentials. It is worth noting, however, that for the redox equilibrium conditions used in this work, the neglect of activity coefficients should be inconsequential because the ionic strength of the medium is particularly low (e.g., $[\text{NMQ}] \leq 4 \times 10^{-4}$ M) and because the activity coefficients of the species on both sides of the equilibrium in eq 1 are expected to be quite similar.

Fitting of the four equilibrium spectra in Figure 2 gave an average value for K_{et} of 0.059(7).²¹ The average value of K_{et} from three independent experiments was 0.057(5). This value of K_{et} corresponds to $E_{\text{ox}}(\text{3}) - E_{\text{ox}}(\text{4}) = 0.071(2)$ V. Note that the error in ΔE_{ox} is small (2 mV) but typical of the high precision that can be obtained by the redox equilibrium method.^{7a} The values of ΔE_{ox} for the remaining pairs of reference compounds were obtained in a similar manner from an average of 3–5 independent experiments, with similarly excellent results (see Supporting Information for equilibrium spectra). A summary of the ΔE_{ox} values for compounds **1–6** is given in Table 1.

(21) The standard deviation in the last significant digit is given in parentheses.

We next sought to compare the relative oxidation potentials derived from the redox equilibrium method to those obtained electrochemically. Fortunately, the oxidation potentials of **1–6** have been all determined electrochemically in CH_2Cl_2 by Gould and co-workers.^{8a} For our later redox equilibrium experiments with arylcyclopropanes described below, we also sought absolute oxidation potentials for the reference compounds. This latter objective requires that one of the reference compounds be used as a redox anchor; we chose **6** because its electrochemical oxidation is well behaved (i.e., fully reversible) and because we wanted to later make comparisons to data in CH_3CN , where $E_{\text{ox}}(\mathbf{6})$ has recently been carefully determined (vide infra). Since **6** has the lowest oxidation potential of all of the reference compounds investigated, naturally, as one progresses up the redox ladder, the errors in the derived oxidation potentials increase due to the propagation of errors in ΔE_{ox} . Nonetheless, the error in the oxidation potential of **1**, the highest compound studied in this work, is still only 0.007 V, reflecting the high precision of the method. As shown in Table 1, the oxidation potentials determined by the redox equilibrium method ($E_{\text{ox}}^{\text{eq}}$) are in excellent agreement with those derived electrochemically.

Since electron-transfer reactions—particularly photoinduced electron-transfer reactions—are commonly performed in polar solvents such as acetonitrile, we decided to also determine $E_{\text{ox}}^{\text{eq}}$ for reference compounds **1–6** in CH_3CN . In addition to providing useful reference oxidation potential data, the high precision of the redox equilibrium method offered an opportunity to probe subtle solvation effects on ΔE_{ox} values. The redox equilibrium experiments were carried out using the same NMQ/PhCH₃ photooxidant system used above, except CH_3CN was substituted for CH_2Cl_2 . The results are summarized in Table 1.

Interestingly, comparison of the oxidation potential differences in CH_2Cl_2 vs CH_3CN show a periodic alternation in the relative magnitudes of ΔE_{ox} along the redox ladder. While the average differences are only ± 20 – 30 mV, they are well outside the experimental errors of the equilibrium measurements. Some insight into the origin of the fluctuations in ΔE_{ox} can be obtained from the oxidation potentials of **1–6** in CH_2Cl_2 vs CH_3CN . The latter values, like the former ones, rest on the use of **6** as a redox anchor. The oxidation potential of **6** in CH_3CN has recently been carefully measured by Amatore and co-workers using fast scan cyclic voltammetry with ultramicroelectrodes.²² These workers also measured $E_{\text{ox}}(\mathbf{4})$ in CH_3CN , and their value agrees well with our estimate based on the value of ΔE_{ox} from the redox equilibrium measurements (see Table 1). Comparably reliable electrochemical estimates of E_{ox} for the other reference compounds in CH_3CN are not available for comparison.

A comparison of the $E_{\text{ox}}^{\text{eq}}$ values in CH_2Cl_2 and CH_3CN shows that the oxidation potentials for the substituted benzenes (**2**, **4**, and **6**) are lower in CH_3CN by 10–20 mV. In contrast, the differences in the oxidation potentials of the biphenyls (**1**, **3**, and **5**) are <4 mV between the two solvents and are indistinguishable within experimental error. A plausible explanation for these results is that the differences in the cation radical solvation energies between CH_3CN and CH_2Cl_2 are greater for the benzene cation radicals than for the biphenyl cation radicals. One would expect a greater solvation energy difference for the benzene cation radicals because of their more charge-localized

Table 2. Absorption Maxima (λ_{max}) and Extinction Coefficients (ϵ) for **1⁺–6⁺** in CH_2Cl_2 and CH_3CN

cation radical	λ_{max}		ϵ^a
	CH_2Cl_2	CH_3CN	
1⁺	670	667	14500 ^b
2⁺	451	447	5300
3⁺	700	700	15000
4⁺	457	450	6100
5⁺	699	690	21000
6⁺	490	488	5100

^a Estimated errors in the extinction coefficients are 5%. ^b Reference 8a.

nature. This hypothesis is supported by the observation that solvent reorganization energies for return electron transfer from ion radical pairs in CH_3CN are greater for substituted benzenes than for substituted biphenyls.^{8a}

As noted above, the NMQ/PhCH₃ photooxidation system generates the same concentration of cation radicals with each laser pulse. Therefore, for each redox pair studied, spectra of the reference cation radicals at the same concentration are generated. Thus, the spectra can also be used to determine the relative extinction coefficients of the cation radicals. The relative extinction coefficients could be combined with the previously determined extinction coefficient of **1⁺** in CH_3CN ^{8a} to provide the absolute extinction coefficients of **2⁺–6⁺** in CH_3CN (see Table 2). The relative extinction coefficients of **1⁺–6⁺** were similarly determined in CH_2Cl_2 . Since none of the cation radical extinction coefficients are accurately known in CH_2Cl_2 , it was not possible to obtain their absolute extinction coefficients as in CH_3CN . However, we observed that, when the reference cation spectra were recorded using the same laser power, the absorbances of **1⁺–6⁺** at their λ_{max} were lower in CH_3CN than in CH_2Cl_2 by a constant amount, 0.82(2). This can be explained by either a lower quantum yield for cation radical formation in CH_3CN or uniformly lower extinction coefficients for **1⁺–6⁺** in CH_3CN . The former hypothesis is more reasonable and is consistent with the expectation that return electron transfer within the NMQ/PhCH₃⁺ geminate pair should be faster in CH_3CN . The return electron transfer is expected to lie in the Marcus inverted region;¹² therefore, the higher solvent reorganization energy of CH_3CN should lead to a greater rate constant for return electron transfer,^{8a} which in turn will lead to a lower quantum yield for separated cation radicals. If the data are interpreted in this manner, they require closely similar extinction coefficients for **1⁺–6⁺** in both CH_3CN and CH_2Cl_2 , since otherwise the ratios of absorbances at λ_{max} would not be expected to be constant. The extinction coefficients are summarized in Table 2, along with λ_{max} for the cation radicals in both CH_2Cl_2 and CH_3CN .

C. Redox Equilibria with Arylcyclopropanes. With the $E_{\text{ox}}^{\text{eq}}$ values for reference compounds **1–6** in hand, redox equilibrium experiments were next carried out with arylcyclopropanes **7–15**. These cyclopropanes were studied because of their relevance to our previous work⁹ and to address uncertainties in the literature oxidation potentials. Experiments were performed in CH_2Cl_2 since the cyclopropane cation radicals react rapidly with CH_3CN .⁹ The optimum choice of reference compound for each cyclopropane was based on maximizing the spectral differences between their respective cation radicals and minimizing ΔE_{ox} of the neutrals. To select a reference compound of similar oxidation potential, the electrochemically determined oxidation potentials of the cyclopropanes were used as an

(22) Amatore, C.; Lefrou, C. *J. Electroanal. Chem.* **1992**, *325*, 239.

Table 3. ΔE_{ox} for **7–15** and Reference Compounds **1–6** Determined from Redox Equilibrium Experiments in CH_2Cl_2 at 20 °C, Oxidation Potentials for **7–15** ($E_{\text{ox}}^{\text{eq}}$) Based on ΔE_{ox} , and Electrochemically Determined Oxidation Potentials for **7–15** (E_{p} and $E_{\text{p}/2}$) in CH_3CN

cyclopropane	reference	ΔE_{ox}	$(E_{\text{ox}}^{\text{eq}})^{\text{a}}$	$(E_{\text{p}})^{\text{b}}$	$(E_{\text{p}/2})^{\text{b}}$
7	1	−0.032(2)	1.918(7)	2.03	1.84, 1.74 ^c
8	1	−0.038(2)	1.912(7)	1.97	1.83, 1.72 ^d , 1.78 ^e
	2	−0.015(2)	1.910(7)		1.83 ^e , 1.87 ^f , 2.34 ^g
9	3	+0.011(4)	1.854(7)	1.95, 2.0 ^h	1.70
10	4	+0.028(3)	1.800(7)	1.80	1.69
11	4	+0.024(4)	1.796(7)	1.79	1.67
12	4	+0.020(3)	1.792(7)	1.81	1.69, 1.71 ^f
13	5	−0.007(4)	1.657(6)	1.70	1.51
14	5	−0.043(7)	1.621(9)		1.75 ⁱ
15	5	−0.039(3)	1.625(6)		1.44 ^f , 1.48 ^j , 1.51 ⁱ
	6	+0.032(5)	1.622(5)		

^a $E_{\text{ox}}^{\text{eq}}$ (reference, CH_2Cl_2) + ΔE_{ox} ; V vs SCE in CH_2Cl_2 ; standard deviation in the last significant digit in parentheses. ^b This work unless otherwise noted; V vs SCE in CH_3CN ; where necessary literature potentials were converted to SCE on the basis of corrections given in ref 31. ^c Reference 32a. ^d Reference 32b. ^e Reference 32c. ^f Reference 32d. ^g Reference 32e. ^h Reference 32f. ⁱ Reference 32g. ^j Reference 32h.

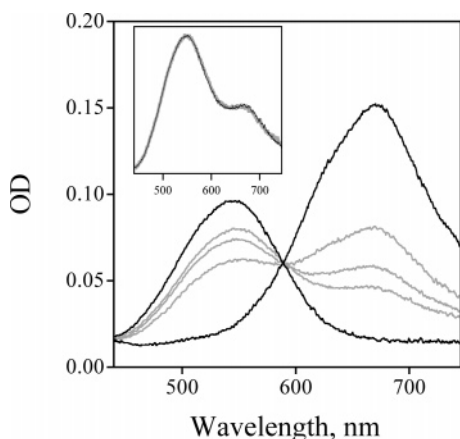


Figure 3. Spectra of phenylcyclopropane radical ($\lambda_{\text{max}} = 540$ nm), biphenyl cation radical ($\lambda_{\text{max}} = 670$ nm), and the corresponding equilibrium, electron-transfer spectra (gray lines) in CH_2Cl_2 . Inset shows one of the experimental spectra (gray line) and the best least-squares fit to it according to eq 2 (thin black line).

approximate guide, but sometimes the best reference compound had to be found by trial and error.

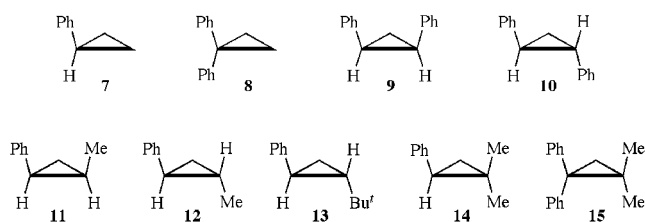


Figure 3 shows data for the redox equilibrium established between phenylcyclopropane (**8**) and biphenyl (**1**). Good equilibrium behavior is evidenced by the clean isosbestic point at ~ 590 nm. Fitting of the equilibrium spectra as described above provided a value for $E_{\text{ox}}(\mathbf{8}) - E_{\text{ox}}(\mathbf{1})$ of $-0.038(2)$ V. Combining this with the oxidation potential of **1** determined earlier provides $E_{\text{ox}}(\mathbf{8}) = 1.912(7)$ V vs SCE. As discussed in the Introduction, literature values for the oxidation potential of **8** ranged from 1.72 to 2.34 V vs SCE. Thus, the redox equilibrium measurements have reduced the uncertainty in the oxidation potential of **8** by a factor of ~ 50 ! The oxidation potentials for the remainder of the cyclopropanes were determined in an analogous manner (see Supporting Information for spectra). The results are listed in Table 3. To test the internal consistency of oxidation

potentials, ΔE_{ox} for cyclopropanes **8** and **15** were each determined against two different reference compounds to obtain two independent estimates of $E_{\text{ox}}^{\text{eq}}$ for each of the cyclopropanes. As the data in Table 3 show, the oxidation potentials derived from different reference compounds are in excellent agreement for both cyclopropanes.

Also shown in Table 3 are the oxidation potentials of the cyclopropanes determined electrochemically by cyclic voltammetry in CH_3CN . Where available, anodic peak potentials (E_{p}) and half-peak potentials ($E_{\text{p}/2}$) are provided. All of the electrochemical oxidations are irreversible, presumably due to rapid follow-up reactions of the cyclopropane cation radicals. As discussed above, arylcyclopropane cation radicals $\mathbf{7}^{+\bullet}$ – $\mathbf{15}^{+\bullet}$ all react with CH_3CN , which is why the redox equilibrium measurements were made in CH_2Cl_2 . Since the electrochemical potentials were all measured in CH_3CN , however, we sought to test the effect of solvent on ΔE_{ox} measured by the redox equilibrium method. By making equilibrium measurements at relatively short times, we found that it was possible to determine ΔE_{ox} for phenylcyclopropane (**8**) and biphenyl (**1**) in CH_3CN . The measured ΔE_{ox} was $-0.054(2)$ V, which provides $E_{\text{ox}}^{\text{eq}}(\mathbf{8}) = 1.899(6)$ V vs SCE in CH_3CN . This value differs from that determined in CH_2Cl_2 by $0.012(9)$ V. $E_{\text{ox}}^{\text{eq}}(\mathbf{8})$ in CH_2Cl_2 vs CH_3CN is ca. one-half of that observed for the alkylbenzenes, consistent with the greater degree of charge delocalization expected for $\mathbf{8}^{+\bullet}$.^{9g} Since the other arylcyclopropane cation radicals should have a greater degree of charge delocalization than $\mathbf{8}^{+\bullet}$,^{9g} the oxidation potentials of the other arylcyclopropanes in CH_2Cl_2 and CH_3CN are expected to be even more similar than for **8**.

Several other aspects of the arylcyclopropane oxidation potentials are worthy of comment. First, previous electrochemical measurements suggested quite different effects of geminal vs vicinal diphenyl substitution on E_{ox} . For example, electrochemical data suggested that the oxidation potential of 1,1-diphenylcyclopropane (**7**) was similar to that of *cis*-1,2-diphenylcyclopropane (**14**) but substantially higher than for *trans*-1,2-diphenylcyclopropane (**15**) (cf. $E_{\text{p}/2}$ values in Table 3). In contrast, the redox equilibrium measurements show that the oxidation potential of **7** is nearly 0.3 V greater than those of *both* **14** and **15**. The lower oxidation potentials of **14** and **15** are consistent with the delocalized structures proposed for $\mathbf{14}^{+\bullet}$ and $\mathbf{15}^{+\bullet}$ on the basis of the CIDNP experiments by Roth and co-workers.²³ It is clear that the electrochemical measurements,

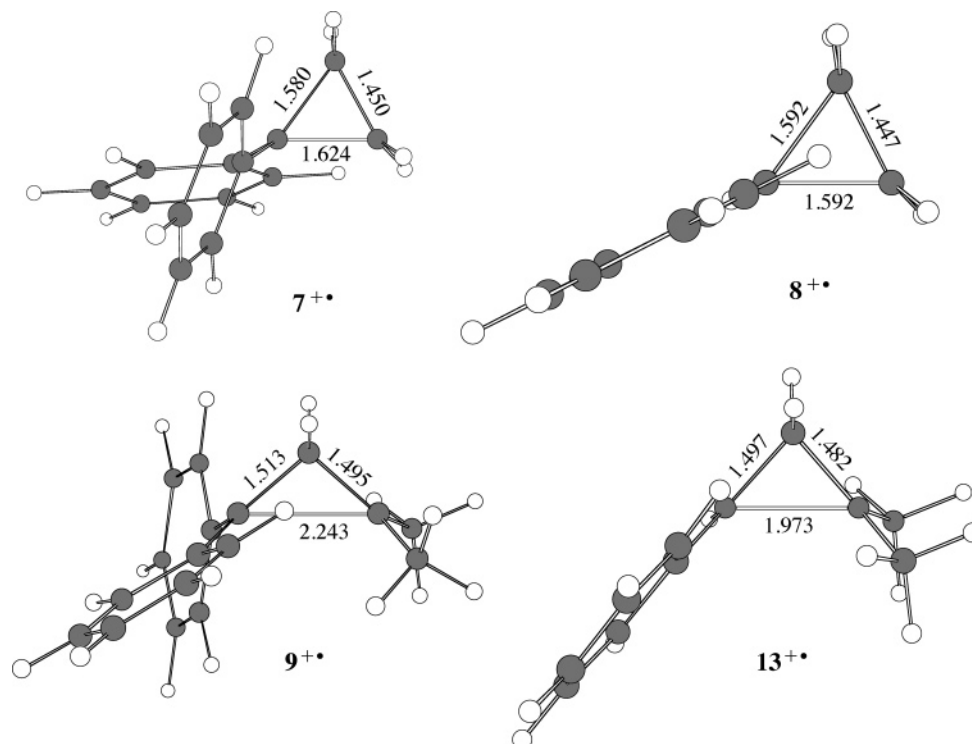


Figure 4. B3LYP/6-311G(d,p) calculated structures and selected bond lengths for cyclopropane cation radicals.

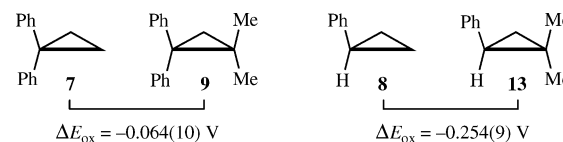
which previously suggested that **14** and **15** had significantly different oxidation potentials, are not supported by the equilibrium oxidation potential measurements.

Similar to the results above, alkyl substitution at C2 also lowers the oxidation potential of phenylcyclopropanes. Thus, the redox-equilibrium-derived oxidation potentials of *cis*- and *trans*-1-phenyl-2-methylcyclopropane (**11** and **12**) are 0.11–0.12 V lower than that of phenylcyclopropane (**8**). The effect of 2-alkyl substitution on E_{ox} is smaller than that of 2-phenyl substitution, suggesting that a methyl group is not as effective as a phenyl group for cation radical stabilization. Note that the oxidation potentials of **11** and **12** are indistinguishable within experimental error. Thus, as with 1,2-diphenylcyclopropanes **14** and **15**, *cis* vs *trans* methyl substitution has no discernible effect on E_{ox} .

The oxidation potential of *trans*-1-phenyl-*tert*-butylcyclopropane (**10**) is also noteworthy. One might have expected the more electron-releasing *tert*-butyl group to cause $E_{ox}(\mathbf{10}) < E_{ox}(\mathbf{12})$, whereas the equilibrium oxidation potential data suggest the opposite. We propose that this surprising result may be the result of steric inhibition of solvation of $\mathbf{10}^{+\bullet}$ (relative to $\mathbf{12}^{+\bullet}$) by the *tert*-butyl group. The similarity in oxidation potentials for **10** and **12** is also supported by electrochemical data (see Table 3), albeit more tenuously.

Perhaps the most striking aspect of the arylcyclopropane oxidation potential measurements relates to the effect of 2,2-dimethyl substitution for 1-phenyl- vs 1,1-diphenylcyclopropanes. As illustrated below, redox equilibrium measurements show that 2,2-dimethyl substitution lowers the oxidation potential ca. 4 times less for 1,1-diphenylcyclopropane than for 1-phenylcyclopropane. It is worth noting that, here, the electrochemical data (Table 3) are ambiguous. While ΔE_p data show

nearly the same difference in $\Delta\Delta E_{ox}$ for **7/9** vs **8/13** as the equilibrium oxidation potential measurements (0.19 V), the $\Delta E_{p/2}$ values show no difference when recorded under the same electrochemical conditions.



The origin of the differences in ΔE_{ox} for **7/9** vs **8/13** can be attributed to structural differences in the cation radicals, especially between $\mathbf{9}^{+\bullet}$ and $\mathbf{13}^{+\bullet}$. The structures of all four cation radicals were computed using the B3LYP density functional method, which is particularly well suited to cation radicals.²⁴ Using a 6-311G(d,p) basis set, cation radicals $\mathbf{7}^{+\bullet}$ and $\mathbf{8}^{+\bullet}$ are both predicted to have nearly equal C1–C2 and C1–C3 bond lengths that are elongated relative to the neutral cyclopropanes; i.e., they have so-called 2L1N (two long, one normal) structures.^{9b} In contrast, $\mathbf{9}^{+\bullet}$ and $\mathbf{13}^{+\bullet}$ are predicted to have 1L2N structures, where the C1–C2 bonds are significantly elongated relative to those in $\mathbf{7}^{+\bullet}$ and $\mathbf{8}^{+\bullet}$. As shown in Figure 4, elongation of the C1–C2 bond in $\mathbf{9}^{+\bullet}$ is significantly greater than that in $\mathbf{13}^{+\bullet}$ ($r_{C1-C2} = 2.24$ for $\mathbf{9}^{+\bullet}$ vs 1.97 Å for $\mathbf{13}^{+\bullet}$). For comparison, the calculated C1–C2 bond lengths in the parent cation radicals $\mathbf{7}^{+\bullet}$ and $\mathbf{8}^{+\bullet}$ differ by <0.03 Å. The large difference in r_{C1-C2} between $\mathbf{9}^{+\bullet}$ and $\mathbf{13}^{+\bullet}$ can be ascribed to differential steric effects. As shown in Figure 4, the phenyl group in $\mathbf{13}^{+\bullet}$ is optimally oriented for overlap with the elongated C1–C2 σ bond. In this conformation, the phenyl group at C1 and the *syn*-methyl group at C2 do not sterically interfere to a significant extent. For $\mathbf{9}^{+\bullet}$, however, neither phenyl group is optimally

(23) (a) Roth, H. D.; Schilling, M. L. M. *J. Am. Chem. Soc.* **1980**, *102*, 7956.
(b) Roth, H. D.; Schilling, M. L. M. *J. Am. Chem. Soc.* **1981**, *103*, 7210.

(24) Bally, T.; Borden, W. T. *Rev. Comput. Chem.* **1999**, *13*, 1.

Table 4. Absorption Maxima (λ_{\max}) and Extinction Coefficients (ϵ) for Arylcyclopropane Cation Radicals **7**⁺–**15**⁺ in CH₂Cl₂.

cation radical	λ_{\max}	ϵ^a
7 ⁺	510	6700
8 ⁺	540	8300
9 ⁺	615	4500
	515	6300
10 ⁺	550	11000
11 ⁺	560	7300
12 ⁺	545	9200
13 ⁺	540	5000
14 ⁺	675	5700
	480	19000
15 ⁺	700	11000
	430	23000

^a Estimated errors in the extinction coefficients are 10%.

oriented for σ – π overlap with the elongated bond. Eclipsing interactions between ortho ring protons of the two phenyl groups in **9**⁺ presumably prevent either ring from achieving the coplanar conformation that would maximize σ – π overlap. The gearing of the phenyl rings in **9**⁺ results in a nonbonded interaction between one of the phenyl rings and the syn-methyl group at C2, which is presumably relieved by elongation of the C1–C2 bond. This additional lengthening of the C1–C2 bond in **9**⁺ raises the energy of the cation radical relative to a hypothetical structure of shorter bond length (more similar to **13**⁺) in which the steric interaction is absent. The increase in the energy of **9**⁺ results in a higher oxidation potential for **9** and thereby decreases the oxidation potential difference between **7** and **9**, consistent with the observed equilibrium oxidation potentials.

Finally, the absorption maxima and extinction coefficients for arylcyclopropane cation radicals **7**⁺–**15**⁺ are given in Table 4. Although the data show that both λ_{\max} and ϵ can be influenced by alkyl and phenyl substitution, a detailed interpretation of the data must await further study into the detailed nature of cation radical electronic transitions, similar to that recently carried out for **8**⁺.²⁵

Summary

A general, nanosecond redox equilibrium method has been developed for determining accurate oxidation potentials in organic solvents for compounds that form short-lived cation radicals. Furthermore, the method can readily provide oxidation potentials with a precision of ≤ 10 mV. The equilibrium method has been successfully tested using a series of substituted arylcyclopropanes, whose oxidation potentials were imprecisely known previously. The generality of the redox equilibrium methodology should permit similarly accurate oxidation potentials to be measured for a variety of other substrates.

Experimental Section

Materials. Methylene chloride was distilled from P₂O₅ under nitrogen. Acetonitrile was purified by passing the solvent over a bed of activated alumina.²⁶ Reference compounds **1**–**6** were purchased in the highest available purity and recrystallized several times before use (solids) or were fractionally distilled (liquids). Cyclopropanes **7**, **10**, **14**, and **15** were prepared by literature methods.²⁷ The remainder of the cyclopropanes were obtained as described previously.^{9a}

(25) Dinocenzo, J. P.; Merchán, M.; Roos, B. O.; Shaik, S.; Zuilhof, H. J. *Phys. Chem. A* **1998**, *102*, 8979.

(26) Pangborn, A. B.; Giardello, M. A.; Grubbs, R. H.; Rosen, R. K.; Timmers, F. J. *Organometallics* **1996**, *15*, 1518. (b) Alaimo, P. J.; Peters, D. W.; Arnold, J.; Bergman, R. G. *J. Chem. Educ.* **2001**, *78*, 64.

Nanosecond Apparatus. A modified version of the nanosecond laser flash apparatus previously described²⁸ was used. Excitations (343 nm; 1–3 mJ/pulse; 7 ns pulses) were performed using a XeCl excimer-pumped dye laser containing *p*-terphenyl. A home-built xenon flashlamp system equipped with a Perkin-Elmer FX-193 flashlamp was used to generate analyzing light. A portion of the analyzing light was focused into the end of a fiber optic cable and, in turn, onto the entrance slit of a Acton Research SpectroPro-275 monochromator equipped with an Oriol Instaspec V gated, intensified CCD.

Equilibrium Measurements. *N*-Methylquinolinium hexafluorophosphate¹¹ solutions (OD ≈ 0.5 at 343 nm) containing 1 M toluene were prepared in methylene chloride or acetonitrile. Experiments were conducted in quartz cuvettes equipped with high-vacuum stopcocks that carried serum caps. Solvent-saturated dioxygen was bubbled through the solutions for 10–15 min before equilibrium measurements were made. Initially, separate solutions were prepared with each of the equilibrium components in order to record the spectra of their corresponding cation radicals. Increasing concentrations of the second component were then added to one of the cuvettes from a dioxygen-saturated stock solution via a calibrated gastight syringe equipped with a 6-in. 22-gauge fixed needle. All equilibrium measurements were made at 20 °C. In general, equilibrium measurements were made 100 ns after the laser pulse. At the end of each equilibrium experiment, the spectrum of the sample containing the single equilibrium component was re-recorded to ensure that the laser power had not changed during the course of the experiment. Equilibrium spectra were fit to eqs 2 and 3 with Igor Pro (version 4.07; Wavemetrics, Inc.). The oxidation potential differences given in Tables 1 and 3 are averages of 3–5 independent determinations for **1**–**6** and 1–3 determinations for **7**–**15**.

Cyclic Voltammetry. Oxidation potentials were measured at room temperature using a BAS-100B/W Electrochemical Workstation using a three-electrode cyclic voltammetry cell. The cell was outfitted with a 1.5-mm-diameter platinum disk working electrode, a platinum gauze auxiliary electrode, and a silver wire reference electrode. All potentials were referenced to internal ferrocene (0.39 V vs SCE).²⁹ Solutions containing ~ 5 mM cyclopropane (**7**–**13**) and 0.1 M tetra-*n*-butylammonium hexafluorophosphate as the supporting electrolyte were prepared in dry acetonitrile under a nitrogen atmosphere. Samples were analyzed using a scan rate of 150 mV/s. At this scan rate, all samples showed irreversible oxidation waves.

(27) (a) **7**: Jorgenson, M. J.; Thacher, A. F. *Org. Synth.* **1968**, *48*, 75. (b) **10**: Casey, C. P.; Polichnowski, S. W.; Shusterman, A. J.; Jones, C. R. *J. Am. Chem. Soc.* **1979**, *101*, 7282. (c) **14**, **15**: Yang, Z.; Lorenz, J. C.; Shi, Y. *Tetrahedron Lett.* **1998**, *39*, 8621.

(28) Shukla, D.; Liu, G.; Dinocenzo, J. P.; Farid, S. *Can. J. Chem.* **2003**, *81*, 744.

(29) Gagné, R. R.; Koval, C. A.; Lisensky, G. C. *Inorg. Chem.* **1980**, *19*, 2854.

(30) Frisch, M. J.; Trucks, G. W.; Schlegel, H. B.; Scuseria, G. E.; Robb, M. A.; Cheeseman, J. R.; Montgomery, J. A., Jr.; Vreven, T.; Kudin, K. N.; Burant, J. C.; Millam, J. M.; Iyengar, S. S.; Tomasi, J.; Barone, V.; Mennucci, B.; Cossi, M.; Scalmani, G.; Rega, N.; Petersson, G. A.; Nakatsuji, H.; Hada, M.; Ehara, M.; Toyota, K.; Fukuda, R.; Hasegawa, J.; Ishida, M.; Nakajima, T.; Honda, Y.; Kitao, O.; Nakai, H.; Klene, M.; Li, X.; Knox, J. E.; Hratchian, H. P.; Cross, J. B.; Adamo, C.; Jaramillo, J.; Gomperts, R.; Stratmann, R. E.; Yazyev, O.; Austin, A. J.; Cammi, R.; Pomelli, C.; Ochterski, J. W.; Ayala, P. Y.; Morokuma, K.; Voth, G. A.; Salvador, P.; Dannenberg, J. J.; Zakrzewski, V. G.; Dapprich, S.; Daniels, A. D.; Strain, M. C.; Farkas, O.; Malick, D. K.; Rabuck, A. D.; Raghavachari, K.; Foresman, J. B.; Ortiz, J. V.; Cui, Q.; Baboul, A. G.; Clifford, S.; Cioslowski, J.; Stefanov, B. B.; Liu, G.; Liashenko, A.; Piskorz, P.; Komaromi, I.; Martin, R. L.; Fox, D. J.; Keith, T.; Al-Laham, M. A.; Peng, C. Y.; Nanayakkara, A.; Challacombe, M.; Gill, P. M. W.; Johnson, B.; Chen, W.; Wong, M. W.; Gonzalez, C.; Pople, J. A. *Gaussian 03*, Revision B.3; Gaussian, Inc.: Pittsburgh, PA, 2003.

(31) Larson, R. C.; Iwamoto, R. T.; Adams, R. N. *Anal. Chim. Acta* **1961**, *25*, 371.

(32) (a) Takahashi, Y.; Ohaku, H.; Nishioka, N.; Ikeda, H.; Miyashi, T.; Gormin, D. A.; Hilinski, E. F. *J. Chem. Soc., Perkin Trans. 2* **1997**, 303. (b) Mizuno, K.; Ogawa, J.; Otsuji, Y. *Chem. Lett.* **1981**, 741. (c) Somich, C.; Mazzocchi, P. H.; Edwards, M.; Morgan, T.; Ammon, H. L. *J. Org. Chem.* **1990**, *55*, 2624. (d) Shono, T.; Matsumura, Y. *J. Org. Chem.* **1970**, *35*, 4157. (e) Wang, Y.; Tanko, J. M. *J. Am. Chem. Soc.* **1997**, *119*, 8201. (f) Nishida, S.; Murakami, M.; Oda, H.; Tsuji, T.; Mizuno, T.; Matsubara, M.; Kikui, N. *J. Org. Chem.* **1989**, *54*, 3859. (g) Wang, P. C.; Arnold, D. R. *Tetrahedron Lett.* **1979**, 2101. (h) Mizuno, K.; Ichinose, N.; Otsuji, Y. *J. Org. Chem.* **1992**, *57*, 1855.

Calculations. Density functional calculations were performed with the Gaussian 03 series of programs.³⁰ All geometries were fully optimized using a 6-311G(d,p) basis set, and all optimized species were determined to be minima by frequency calculations.

Acknowledgment. Research support was provided by a grant from the National Science Foundation (Grant No. CHE-9812719). G.G. is pleased to acknowledge support for a postdoctoral fellowship from the Ministerio de Educación, Cultura y Deporte de España. H.Z. is grateful to the Netherlands

Organization for Scientific Research (NWO) for a postdoctoral Talent-stipendium.

Supporting Information Available: Sixteen figures of representative equilibrium electron-transfer spectra for **1–15**, and Gaussian archive files for density functional calculations. This material is available free of charge via the Internet at <http://pubs.acs.org>.

JA046946G